

Video Article

Evolution of Staircase Structures in Diffusive Convection

Shuang-Xi Guo¹, Sheng-Qi Zhou¹, Xian-Rong Cen¹, Yuan-Zheng Lu¹

¹State Key Laboratory of Tropical Oceanography, South China Sea Institute of Oceanology, Chinese Academy of Sciences

Correspondence to: Sheng-Qi Zhou at sqzhou@scsio.ac.cn

URL: <https://www.jove.com/video/58316>

DOI: [doi:10.3791/58316](https://doi.org/10.3791/58316)

Keywords: Environmental Sciences, Issue 139, Stratified Fluid, Diffusive Convection, Staircase Structure, Shadowgraph Technique, Convecting Layer, Interface

Date Published: 9/5/2018

Citation: Guo, S.X., Zhou, S.Q., Cen, X.R., Lu, Y.Z. Evolution of Staircase Structures in Diffusive Convection. *J. Vis. Exp.* (139), e58316, doi:10.3791/58316 (2018).

Abstract

Diffusive convection (DC) occurs when the vertical stratified density is controlled by two opposing scalar gradients that have distinctly different molecular diffusivities, and the larger- and smaller- diffusivity scalar gradients have negative and positive contributions for the density distribution, respectively. The DC occurs in many natural processes and engineering applications, for example, oceanography, astrophysics and metallurgy. In oceans, one of the most remarkable features of DC is that the vertical temperature and salinity profiles are staircase-like structure, composed of consecutive steps with thick homogeneous convecting layers and relatively thin and high-gradient interfaces. The DC staircases have been observed in many oceans, especially in the Arctic and Antarctic Oceans, and play an important role on the ocean circulation and climatic change. In the Arctic Ocean, there exist basin-wide and persistent DC staircases in the upper and deep oceans. The DC process has an important effect on diapycnal mixing in the upper ocean and may significantly influence the surface ice-melting. Compared to the limitations of field observations, laboratory experiment shows its unique advantage to effectively examine the dynamic and thermodynamic processes in DC, because the boundary conditions and the controlled parameters can be strictly adjusted. Here, a detailed protocol is described to simulate the evolution process of DC staircase structure, including its generation, development and disappearance, in a rectangular tank filled with stratified saline water. The experimental setup, evolution process, data analysis, and discussion of results are described in detail.

Video Link

The video component of this article can be found at <https://www.jove.com/video/58316/>

Introduction

Double diffusive convection (DDC) is one of the most important vertical mixing processes. It occurs when the vertical density distribution of the stratified water column is controlled by two or more scalar components gradients of opposite directions, where the components have distinctly different molecular diffusivities¹. It widely occurs in oceanography², the atmosphere³, geology⁴, astrophysics⁵, material science⁶, metallurgy⁷, and architectural engineering⁸. DDC is present in almost half of the global ocean, and it has important effects on oceanic multi-scale processes and even climatic changes⁹.

There are two primary modes for DDC: salt finger (SF) and diffusive convection (DC). SF occurs when a warm, salty water mass overlies cooler, fresher water in the stratified environment. When the warm and salty water lies below the cold and fresh water, the DC will form. The remarkable feature of the DC is that the vertical profiles of temperature, salinity and density are staircase-like, composed by alternant homogeneous convecting layers and thin, strongly stratified interfaces. DC mainly occurs in high latitude oceans and some interior salt lakes, such as the Arctic and Antarctic Oceans, the Okhotsk Sea, the Red Sea and African Kivu Lake¹⁰. In the Arctic Ocean, there exist basin-wide and persistent DC staircases in the upper and deep oceans^{11,12}. It has an important effect on diapycnal mixing in the upper ocean and may significantly influence the ice-melting, which recently arouses more and more interests in the oceanography community¹³.

The DC staircase structure was first discovered in the Arctic Ocean in 1969¹⁴. After that, Padman & Dillon¹⁵, Timmermans *et al.*¹¹, Sirevaag & Fer¹⁶, Zhou & Lu¹², Guthrie *et al.*¹⁷, Bebieva & Timmermans¹⁸, and Shibley *et al.*¹⁹ measured the DC staircases in different basins of the Arctic Ocean, including the vertical and horizontal scales of the convecting layer and interface, the depth and total thickness of the staircase, the vertical heat transfer, the DC processes in mesoscale eddy and the temporal and spatial changes of the staircase structures. Schmid *et al.*²⁰ and Sommer *et al.*²¹ observed the DC staircases by using a microstructure profiler in Kivu Lake. They reported the main structure features and heat fluxes of DC and compared the measured heat fluxes with the existing parametric formula. With computer processing speeds improving, the numerical simulations of DC have recently been done, for example, to examine the interface structure and instability, heat transfer through interface, layer merging event, and so on^{22,23,24}.

Field observation has greatly enhanced the understanding of ocean DC for oceanographers, but the measurement is strongly limited by indeterminate oceanic flow environments and instruments. For example, the DC interface has an extremely small vertical scale, thinner than 0.1 m in some lakes and oceans²⁵, and some special high-resolution instruments are needed. The laboratory experiment shows its unique advantages in exploring the fundamental dynamic and thermodynamic laws of DC. With a laboratory experiment, one can observe the evolution of the DC staircase, measure the temperature and salinity, and propose some parameterizations for the oceanic applications^{26,27}. Furthermore,

in a laboratory experiment, the controlled parameters and conditions are readily adjusted as required. For example, Turner first simulated the DC staircase in the laboratory in 1965 and proposed a heat transfer parameterization across the diffusive interface, which was frequently updated and extensively used in the *in situ* oceanic observations²⁸.

In this paper, a detailed experimental protocol is described to simulate the evolution process of the DC staircase, including the generation, development and disappearance, in stratified saline water heated from below. The temperature and salinity are measured by a micro-scale instrument as well as the DC staircases being monitored with the shadowgraph technique. The experimental setup, evolution process, data analysis, and discussion of results are described in detail. By altering the initial and boundary conditions, the present experimental setup and method can be used to simulate other oceanic phenomena, such as the oceanic horizontal convection, deep-sea hydrothermal eruptions, surface mixed layer deepening, the effect of submarine geothermal on ocean circulation, and so on.

Protocol

1. Working Tank

Note: The experiment is carried out in a rectangular tank. The tank includes top and bottom plates and a side wall. The top and bottom plates are made of copper with electroplated surfaces. There is a water chamber within the top plate. An electric heating pad is inserted in the bottom plate. The side wall is made of transparent Plexiglas. The tank size is $L_x = 257$ mm (length), $L_y = 65$ mm (width) and $L_z = 257$ mm (height). The thickness of the sidewall is 9.5 mm.

1. Clean the copper plates and the Plexiglas sidewall carefully with distilled water.
2. Assemble the tank with screws to ensure that the tank is water-tight.
3. Set up a stainless-steel supporting frame (height of 150 mm) on an optical table and fix the tank above the frame with a heat insulating slab in between, which limits the heat leakage from the working tank to the table.
4. Insert three thermistors (temperature stability of 0.01 °C) into each plate and connect them to a digital multimeter. Note these thermistors are used to monitor the temperatures of the top and bottom plates.
5. Place a Micro-Scale Conductivity and Temperature Instrument (MSCTI) inside the tank and connect it to a Multifunction Data Acquisition (MDA). Fix the MSCTI to a Motorized Precision Translation Stage (MPTS).
Note: Note that the MSCTI can be moved up and down by the vertically moving, so that the temperature and salinity profiles of the working fluid are achieved. Here, the MSCTI has temperature stability of 0.01 °C and salinity stability of 1%. The MPTS has positional accuracy of 0.005 mm.
6. Set the parameters in corresponding software programs of the Digital Multimeter and the Multifunction Data Acquisition, such as sampling rates, data acquisition channels and storage paths. Here, set the sampling rates of the digital Multimeter and the Multifunction Data Acquisition as 1.0 and 128 Hz, respectively.
7. Set the moving parameters in the software program of the MPTS, including the initial position, the lowest and highest positions, moving speed and acceleration, of the MSCTI. Here, set the moving speed and acceleration as 1 mm/s and 0.5 mm/s², and set the lowest and highest positions as 20 and 220 mm above the bottom plate. This leads to a time period of the MPTS of 404 s for an up-down measurement. Set the initial position of the MSCTI at the lowest position.
8. Keep the room temperature almost constant around 24 °C with two high-power air conditioners (working power of 3000 W).

2. Optical Apparatus

Note: During the experiment, the evolution of the DC staircase would be monitored with the shadowgraph technique, which is fulfilled with the below procedures

1. Attach a piece of tracing paper (25.7 cm x 25.7 cm) on the outside of the tank.
2. Use a narrow beam LED lamp as the light source. Place the light source about 5 m away from the other side of the tank, so that a nearly collimated light can be generated. Note that during the experiment the DC layered fluid structure is illuminated on the tracing paper because of the density change (corresponding to the change of index of refraction) of the fluid.
3. Place a high-speed camcorder on the same side of the tracing paper. It is about 1 m away from the tank so that the layered structures with the full-size tank can be recorded.
4. Set the sampling rate of the camcorder. Note that the sampling rate should be proper to capture the detail of the staircase evolutions. Here, the sampling rate of the camcorder is 25 Hz.
5. Turn on the lamp and camcorder, and slightly adjust their positions and distances, to ensure that clear images can be captured by the camcorder.

3. Working Fluid

1. Prepare the saline and fresh waters in two tanks.
 1. Join two identical rectangular tanks (tank A and tank B) by a flexible tube (10 cm in length, 6 mm in inner diameter and 10 mm in outer diameter) from the bottom of each one.
 2. Fill tank A with saline water, its mass concentration of salt (*i.e.*, salinity) is 60 g/kg in this example.
 3. Fill the tank B with an equal volume of de-gassed fresh water, and use an electric magnetic stirrer to continuously homogenize the fluid.
 4. Keep the initial fluid temperature within both tanks the same as the room temperature (24 °C).
2. Establish linear density stratification in the working tank.
 1. Use the double-tank method²⁹ to establish an initial linear stratification of the saline water in the working tank.

- Place tank A and B at the same height, which is 30 cm higher than the working tank. Join tank B and the working tank with another flexible tube (50 cm in length, 2 mm in inner diameter and 5 mm in outer diameter) from their bottoms. Due to the fluid pressure difference in these two tanks, the fluid in tank B can be slowly injected into the working tank.
- Control the flow speed with a peristaltic pump at 0.45 mL/s. Note the whole time of water-filling for the working tank is about 3 h. Calculate the salinity at the bottom of the working tank based on²⁹

$$S_B = S_A \frac{V}{2V_0} \quad (1)$$

where S_A , V and V_0 are salinity of tank A, the final fluid volume of the working tank and the initial fluid volume of tank A (or B), respectively. Using the salinity at the bottom S_B and the fresh water at the top, the buoyancy frequency of initial stratification N_0 is

$$N_0 = \sqrt{\frac{g}{\rho_0} \frac{d\rho}{dz}} = \sqrt{g\beta \frac{dS}{dz}} = \sqrt{g\beta \frac{S_B}{L_z}} \quad (2)$$

where g is gravitational acceleration, ρ_0 is reference density and β is salinity contraction coefficient. Note the N_0 is calculated as 1.14 rad/s in this example.

4. Running the Experiment

- Set the boundary conditions for the working tank.
 - Connect the water chamber of the top plate to a refrigerated circulator with eight uniformly distributed plastic soft tubes (150 cm in length, 10 mm in inner diameter and 15 mm in outer diameter). Note that the temperature of the top plate depends on the temperature of the refrigerated circulator. Set the temperature of the top plate to be the same as the room temperature (24 °C).
 - Connect the electric heating pad inside the bottom plate to a Direct-Current Supply. Note a constant heat flux is provided to the working fluid during this experiment, which is calculated as

$$F_h = \frac{U^2}{RA} \quad (3)$$

where U , R , and A are the supplied voltage, electric resistance and effective area of the electric heating pad, respectively. In this example, the resistance and effective area are 44.12 ohm and $1.89 \times 10^{-2} \text{ m}^2$. Set the supplied voltage as 60 V, so that the total heat flux F_h is 4317 W/m².

- Turn on the camcorder to record the flow pattern.
 - Turn on the Digital Multimeter, Multifunction Data Acquisition to monitor the temperature of the top and bottom plates and the temperature and salinity of fluid using the MSCTI.
 - Turn on the MPTS to move the MSCTI up and down to achieve the temperature and salinity profiles of the working fluid.
 - Turn on the refrigerated circulator and the Direct-Current Supply to achieve the top and bottom boundary conditions of the working fluid.
- Note: Note that the whole experiment will experience the generation, development, mergence, and disappearance of the DC staircase, and it will last about 5 hours. After the disappearance of all DC staircases, turn off the Direct-Current Supply, Refrigerated Circulator, MPTS, Digital Multimeter, Multifunction Data Acquisition, and camcorder in turn.

5. Data Processing

- Shadowgraph image
 - Use a Matlab program to convert the video recorded by the camcorder to successive images for further analysis. Tailor these images to accentuate the flow pattern within the tank. Set the digital image intensity as $I(x, z)$, where (x, z) denotes the horizontal and vertical coordinates with the origin at the bottom-left corner of the image. Note $I(x, z)$ varies over (0, 1) with gray level of 256. Normalize each image by a background image as³⁰

$$\tilde{I}_i(x, z) = \frac{I_i(x, z)}{I_0(x, z)} - 1 \quad (4)$$

where $I_0(x, z)$ is the average image intensity over 10 images taken before the cooling and heating being applied, $I_i(x, z)$ denotes the intensity of the i th image. In this way, the stationary defects in the images can be removed. In order to examine the temporal evolution of DC pattern, each image can be converted to a single vertical intensity fluctuation profile, $\delta I(z)$, by calculating the image intensity fluctuation (*i.e.*, root-mean-square of intensity) along the horizontal direction $\delta I(z)$. Plot the intensity fluctuation profiles $\delta I(z)$ of the successive images together with increasing time to show the evolutions of the DC staircases.

- Temperature and salinity profiles
 - Note in this experiment the vertical profiles of temperature and salinity of the working fluid are measured by the up-down moving MSCTI. Calculate the temporal height, $h(t)$, of the MSCTI with the mean moving speed w , time t , the starting time t_0 (corresponding to the lowest position), the lowest position h_L and highest position h_H , as

$$\frac{(t-t_0)}{t_p} = n + \delta \quad (5)$$

where $t_p = (h_H - h_L)/w$ is the MSCTI moving period from lowest (highest) to highest (lowest) position, n and δ are the integral and fractional parts, respectively. Then calculate the temporal height $h(t)$ as

$$h(t) = \begin{cases} h_L + \delta(h_H - h_L) & \text{if } n \text{ is even} \\ h_H - \delta(h_H - h_L) & \text{if } n \text{ is odd} \end{cases} \quad (6)$$

Note in Equation (6), if n is even, the MSCTI is moving up; otherwise the MSCTI is moving down. Plot the time series temperature $T(t)$ and salinity $S(t)$ in terms of height $h(t)$ to get the vertical temperature and salinity profiles.

Representative Results

Figure 1 shows the schematic of the experimental setup. Its components are described in the protocol. The main parts are shown in **Figure 1a** and the detailed working tank is shown in **Figure 1b**. **Figure 2** shows the temperature changes at the bottom (T_b , the red curve) and top (T_t , the black curve) plates. It is indicated that the temperature of the two plates are almost the same as the room temperature (24 °C) initially. At $t = 641$ s, the top-cooling and bottom-heating are applied. Then, T_b begins to increase rapidly, from 24 °C to 57 °C, while T_t is almost constant until the time reaches 7683 s. During this time range, it is expected that the heating is transferred upwards to the fluid, but has not reached the top plate. At approximately $t = 8000$ s, T_b achieves its maximum, 57 °C, and T_t begins to increase gradually, which implies that the bottom heating reaches the top plate. From then on, the whole tank is completely full of DC staircase structures. Then the bottom-plate temperature begins to decrease and the top-plate temperature continues to increase. At approximately $t = 14800$ s, both T_b and T_t change abruptly, which corresponds to the disappearance of the last interface within the tank. Subsequently, both T_b and T_t approach constant values, where the whole steady flow state belongs to Rayleigh–Bénard convection²⁶.

Figure 3a shows an instantaneous shadowgraph image taken at $t = 3375$ s. There are three interfaces and three convecting layers in the tank. In the convecting layer, the fluid density is homogeneous, while in the interface, large density (or index of refraction) gradient exists, which produces strong light intensity fluctuation. **Figure 3b** shows the intensity fluctuation profile $\delta I(z)$, where the positions of $\delta I(z)$ peaks are corresponding to those of the interfaces. **Figure 3c** shows the intensity fluctuation profile $\delta I(z)$ of shadowgraph image as a function of time $\delta I(z)$. It exhibits the temporal evolution of the DC staircase in the experiment, accompanied with dynamic processes, *i.e.* the layer generation, development, and disappearance. Once the system is heated, a convecting layer forms and thickens gradually from the bottom of system. A sharp interface lies between the convecting layer and the above static fluid. When the bottom convecting layer reaches a certain thickness, a new convecting layer forms above the interface. Meanwhile, the convecting layers and interfaces migrate upward. A similar process continues until a new convecting layer forms above the uppermost interface. In the evolution process, two adjacent layers may merge, or one layer is eroded by another one. At about $t = 8000$ s, the whole tank is occupied by seven convecting layers. Henceforth, the layer merging is the only process and the number of layers gradually reduces. At about $t = 14800$ s, only a single convecting roll exists in the entire tank after the last interface disappears, and the convective flow state approach a stable Rayleigh–Bénard convection. As shown in **Figure 2** and **Figure 3c**, the temperature variances of the top and bottom plates are corresponding to the dynamic changes of the staircases. The recorded temperature and salinity profiles are shown in **Figure 4**. Note that the temperature and salinity profiles are continuously shifted by 1.5 °C, and 3.0 g/kg, respectively, for better clarify. The time interval between two neighbor profiles is 404 s. In this figure, these profiles clearly exhibit the dynamics changes of the staircase structures. The patterns of the staircases are corresponding with layers and interfaces recorded in the shadowgraph measurements (**Figure 3c**).

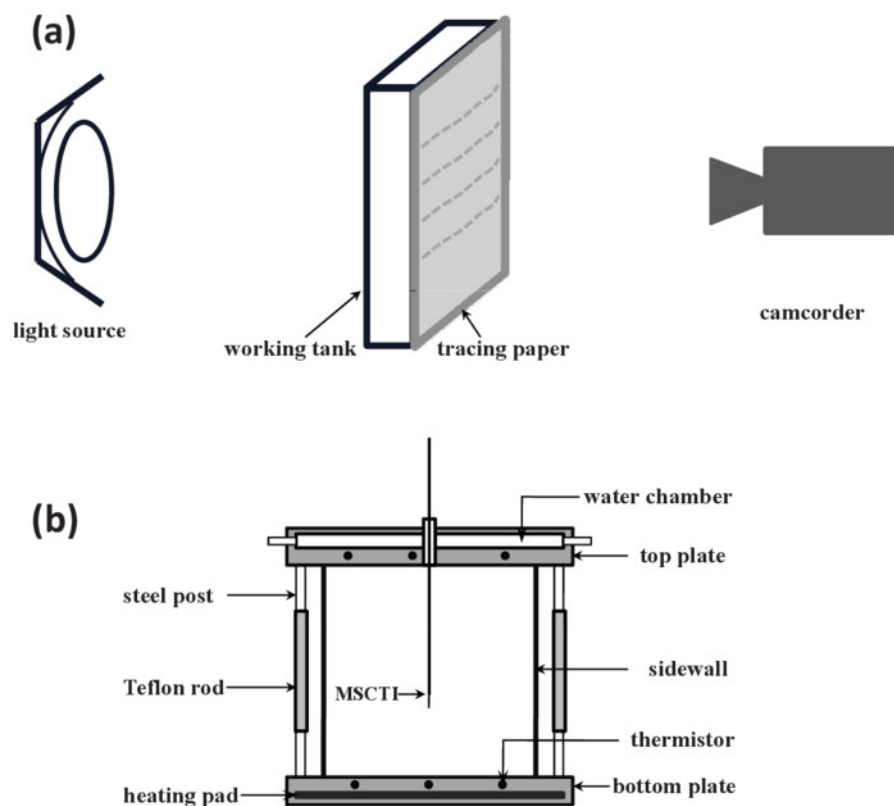


Figure 1. Schematic of the experimental setup (a) Main component parts of the experimental setup. (b) Setup of the working tank. [Please click here to view a larger version of this figure.](#)

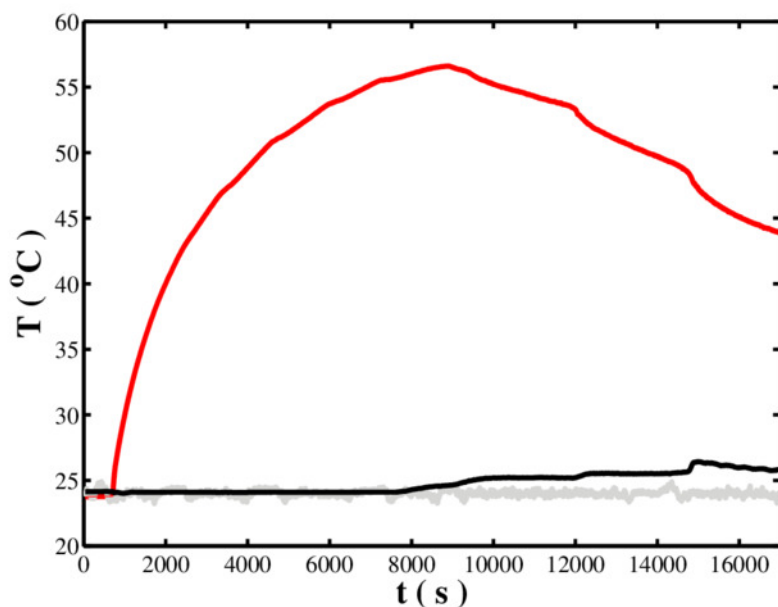


Figure 2. Temperature changes at the bottom (red curve) and top (black curve) plates during the experiment. The gray curve denotes the environment temperature. [Please click here to view a larger version of this figure.](#)

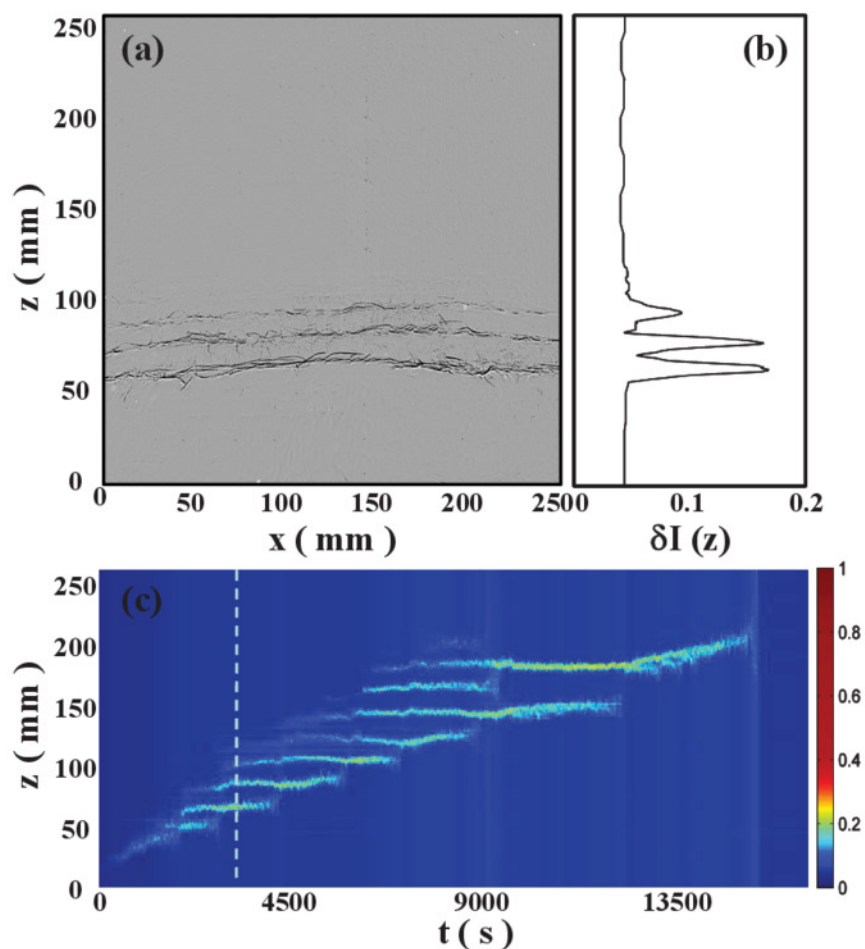


Figure 3. Instantaneous shadowgraph image and post-processing (a) Shadowgraph image at $t=3375$ s, (b) Intensity fluctuation along z direction, $\Delta I(z)$, of the image intensity in **Figure 3a**, (c) Temporal evolution of DC pattern with color shading showing $\Delta I(z)$. The white dashed line corresponds to profile shown in **Figure 3b**. [Please click here to view a larger version of this figure.](#)

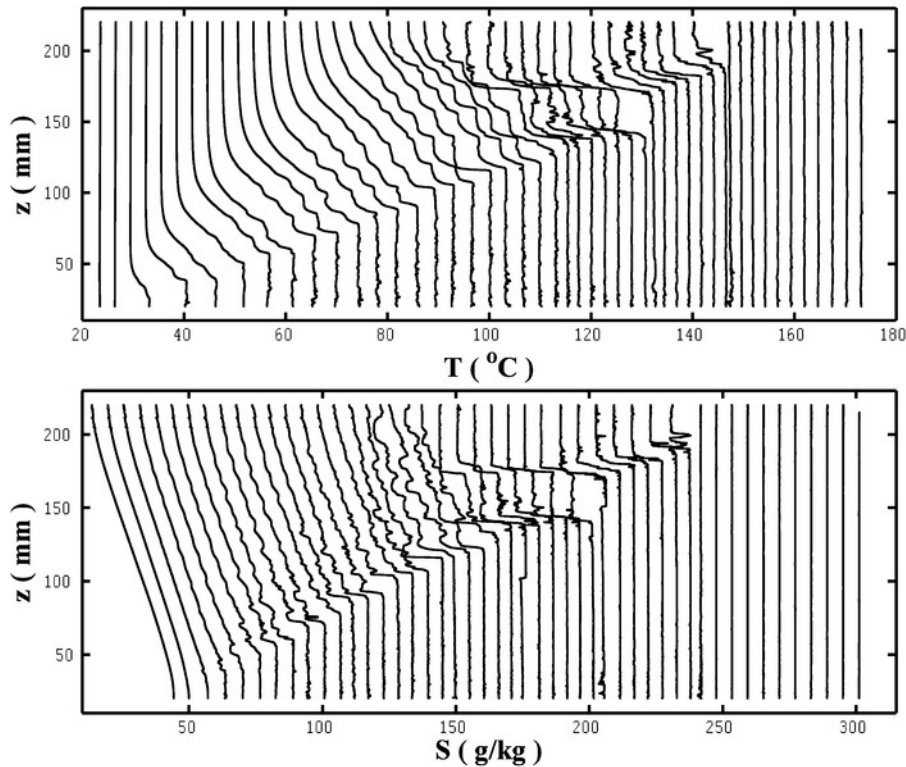


Figure 4. Successive DC evolution profiles. Top: Temperature profiles, Bottom: Salinity profiles. Increments of temperature by 1.5 °C, and salinity by 3.0g/kg between the neighboring profiles are applied. The time interval between two neighbor profiles is 404 s. [Please click here to view a larger version of this figure.](#)

Discussion

In this paper a detailed experimental protocol is described to simulate the thermohaline DC staircase structures in a rectangular tank. An initial linear density stratification of working fluid is constructed using the two-tank method. The top plate is kept at a constant temperature and the bottom one at constant heat flux. The whole evolution process of the DC staircase, including its generation, development, mergence, and disappearance, are visualized with the shadowgraph technique, and the variances of the temperature and salinity are recorded by a high-accuracy probe. With these measurements, one can not only qualitatively observe the changes of staircase, but also quantitatively analyze the changes of temperature, salinity, and density. Furthermore, the variances of layer thickness and heat flux can be parameterized for *in situ* oceanic applications^{26,27}. Some representative experimental results are shown and discussed with the figures.

In step 3.2, the Tank A, Tank B and the working tank are connected during the establishment of the initial linear density stratification for the working tank. By the law of the connected vessels, the fluid in the tank A automatically flows into the tank B, and the flow rate from the tank B into the work tank is precisely twice that from the tank A into the tank B, which can result in a vertically linear density gradient of the working fluid²⁹. In step 5.1, the position of each interface could be identified based on the local maximum intensity fluctuation of the profile $\delta I(z)$; this is because there are strong light intensity fluctuations at the positions of the DC interfaces.

Compared with previous DC experiments in the literature, the present setup and method can measure the temperature and salinity profiles and record the fluid-pattern images synchronously. The temporal and spatial resolutions are high enough to capture the thin interfaces as well as other fine turbulent structures. The main limitation of this method is that the heat exchange between the inside and outside of the working tank has not been recorded, which will be further improved if the accurate vertical heat flux need to be measured.

It is worth to point out that in this experiment the initial density stratification and boundary conditions can readily be controlled as required for different purposes. Some complex working conditions can also be achieved with slightly adjustment, for example the nonlinear stratification can be constructed by modulating the ratio of flow rates from tank A to tank B and that from tank B to the working tank in the two-tank methods²⁹. Therefore, it is expected that the present experimental setup and method could be applied to simulate some other oceanic phenomena, such as the oceanic horizontal convection, deep-sea hydrothermal eruptions, surface mixed layer deepening, and effect of submarine geothermal on ocean circulation, and so on.

Disclosures

The authors have nothing to disclose.

Acknowledgements

This work was supported by the Chinese NSF grants (41706033, 91752108 and 41476167), Grangdong NSF grants (2017A030313242 and 2016A030311042) and LTO grant (LTOZZ1801).

References

1. Turner, J. S. *Buoyancy Effects in Fluids*. 367, Cambridge Univ. Press, N. Y (1973).
2. Schmitt, R.W. Double diffusion in oceanography. *Annual Review of Fluid Mechanics*. **26**, 255-285 (1994).
3. Turner, J.S., and Gustafson, L.B. Fluid motions and compositional gradients produced by crystallization or melting at vertical boundaries. *Journal of Volcanology and Geothermal Research*. **11**, 9S125 (1981).
4. Robb, L. *Introduction to Ore-forming Processes*. Blackwell Publishing, 373 (2004).
5. Chabrier, G., and Baraffe, I. Heat transport in giant (exo)planets: a new perspective. *The Astrophysical Journal Letters*. **661**, 81-84 (2007).
6. Langlois, W.E. Buoyancy-driven flows in crystal-growth melts. *Annual Review of Fluid Mechanics*. **17**, 191 (1985).
7. Chen, C.-F., and Johnson, D. H. Double-diffusive convection: A report on an engineering foundation conference. *Journal of Fluid Mechanics*. **138**, 405-416 (1984).
8. Griffiths, R.W. Layered double-diffusive convection in porous media. *Journal of Fluid Mechanics*. **102**, 221-248 (1981).
9. You, Y. Z. A global ocean climatological atlas of the Turner angle: implications for double-diffusion and water-mass structure. *Deep Sea Research Part I: Oceanographic Research Papers*. **49**, 2075-2093 (2002).
10. Kelley, D.E., Fernando, H.J.S., Gargett, A.E., Tanny, J., and Ozsoy, E. The diffusive regime of double diffusive convection. *Progress in Oceanography*. **56**, 461-481 (2003).
11. Timmermans M.L., Toole, J., Krishfield, R., and Winsor, P. Ice-Tethered Profiler observations of the double-diffusive staircase in the Canada Basin thermocline. *Journal of Geophysical Research: Oceans*. **113**, C00A02, 1-10 (2008).
12. Zhou, S. Q., and Lu, Y. Z. Characterization of double diffusive convection steps and heat budget in the deep Arctic Ocean. *Journal of Geophysical Research: Oceans*. **118** (12), 6672-6686 (2013).
13. Turner, J. S. The melting of ice in the arctic ocean: The influence of double-diffusive transport of heat from below. *Journal of Physical Oceanography*. **40**, 249-256 (2010).
14. Neal, V. T., Neshyba, S. and Denner, W. Thermal stratification in the Arctic Ocean. *Science*. **166** (3903), 373-374 (1969).
15. Padman, L., and Dillon, T. M. Vertical heat fluxes through the Beaufort Sea thermohaline staircase. *Journal of Geophysical Research: Oceans*. **92** (C10), 10799-10806 (1987).
16. Sirevaag, A., and Fer, I. Vertical heat transfer in the Arctic Ocean: The role of double-diffusive mixing. *Journal of Geophysical Research: Oceans*. **117** (C7) (2012).
17. Guthrie, J. D, Fer, I., and Morison, J. Observational validation of the diffusive convection flux laws in the Amundsen Basin, Arctic Ocean. *Journal of Geophysical Research: Oceans*. **120** (12), 7880-7896 (2015).
18. Bebieva, Y., and Timmermans, M. L. An examination of double-diffusive processes in a mesoscale eddy in the Arctic Ocean. *Journal of Geophysical Research: Oceans*. **121** (1), 457-475 (2016).
19. Shibley, N. C., Timmermans, M. L., Carpenter, J. R., and Toole, J. M. Spatial variability of the Arctic Ocean's double-diffusive staircase. *Journal of Geophysical Research: Oceans*. **122** (2), 980-994 (2017).
20. Schmid, M., and Busbridge, M. Double-diffusive convection in Lake Kivu. *Limnology and Oceanography*. **55** (1), 225-238 (2010).
21. Sommer, T., et al. Interface structure and flux laws in a natural double-diffusive layering. *Journal of Geophysical Research: Oceans*. **118** (11), 6092-6106 (2013).
22. Carpenter, J. R., Sommer, T., and Wüest, A. Simulations of a double-diffusive interface in the diffusive convection regime. *Journal of Fluid Mechanics*. **711**, 411-436 (2012).
23. Flanagan, J. D., Lefler, A. S., and Radko, T. Heat transport through diffusive interfaces. *Geophysical Research Letters*. **40** (10), 2466-2470 (2013).
24. Radko, T., Flanagan, J. D., Stellmach, S., and Timmermans, M. L. Double-diffusive recipes. Part II: Layer-merging events. *Journal of Physical Oceanography*. **44** (5), 1285-1305 (2014).
25. Scheifele, B., Pawlowicz, R., Sommer, T., and Wüest, A. Double diffusion in saline Powell Lake, British Columbia. *Journal of Physical Oceanography*. **44** (11), 2893-2908 (2014).
26. Guo, S. X., Zhou, S. Q., Qu, L., and Lu, Y. Z. Laboratory experiments on diffusive convection layer thickness and its oceanographic implications. *Journal of Geophysical Research: Oceans*. **121** (10), 7517-7529 (2016).
27. Guo, S. X., Cen, X. R., and Zhou, S. Q. New parametrization for heat transport through diffusive convection interface. *Journal of Geophysical Research: Oceans*. **123** (2), 1327-1338 (2018).
28. Turner, J. S. The coupled turbulent transports of salt and heat across a sharp density interface. *International Journal of Heat and Mass Transfer*. **8** (5), 759-767 (1965).
29. Hill, D. F. General density gradients in general domains: the "two-tank" method revisited. *Experiments in Fluids*. **32** (4), 434-440 (2002).
30. Zhou, S. Q., and Ahlers, G. Spatiotemporal chaos in electroconvection of a homeotropically aligned nematic liquid crystal. *Physical Review E*. **74** (4), 046212 (2006).